J Appl Electrochem (2007) 37:1463–1474
DOI 10.1007/s10800-007-9369-2

ORIGINAL PAPER

Physical and electrochemical characterization of catalysts for oxygen reduction in fuel cells

C. Christenn · G. Steinhilber · M. Schulze · K. A. Friedrich

Received: 13 November 2006 / Revised: 4 July 2007 / Accepted: 5 July 2007 / Published online: 27 July 2007
© Springer Science+Business Media B.V. 2007

Abstract The cathode catalysts in low temperature fuel cells are associated with major cell efficiency losses, because of kinetic limitations of the oxygen reduction reaction. Additionally, methanol oxidation at the cathode leads to significant lowering of the efficiency in direct methanol fuel cells, which can be alleviated by use of methanol-tolerant catalysts. In this work, alternative carbon-supported platinum-alloy catalysts were investigated by physical methods. Second, methanol-tolerant ruthenium-selenide catalysts were characterized by physical and electrochemical methods. Besides *V–i* characteristics and electrochemical impedance spectroscopy as electrochemical methods, physical methods such as X-ray photoelectron spectroscopy, nitrogen adsorption, porosimetry by mercury intrusion and temperature programmed reduction are used to characterize the catalysts. The electrochemical characterization yields information about properties and behavior of the catalyst. In contrast to platinum a significantly different hydrophobic behavior of the RuSe/C catalysts is found. Low open circuit voltage values measured for RuSe/C indicate an effect on both electrodes. The anode reaction was also influenced by the different cathode catalysts. As a result of the formation of H_2O_2 at the cathode, which passes through the membrane from cathode to anode side, a mixed anode potential is formed. By comparing RuSe/C catalysts before and after electrochemical stressing, changes of the catalysts are determined. Postmortem surface analysis (by X-ray photoelectron spectroscopy) revealed that catalyst composition and MEA structure changed during electrochemical stressing. During fuel cell operation selenium oxide is removed from the surface of the catalysts to a large extent. Additionally, a segregation effect of selenium in RuSe to the surface is identified.

Keywords Cathode catalyst · Electrochemical characterization · Methanol · Pt-alloy · Physical characterization · Ruthenium selenides

C. Christenn (✉) · G. Steinhilber · M. Schulze · K. A. Friedrich
German Aerospace Center, Institute of Technical Thermodynamics, Pfaffenwaldring 38-40, 70569 Stuttgart, Germany
e-mail: Claudia.Christenn@dlr.de

1 Introduction

In order to improve the efficiency of current generation in direct methanol fuel cells (DMFCs), several problems must be solved. For the anode more efficient catalysts are needed, which oxidize electrochemically at lower overpotentials. However, even with more efficient anode catalysts substantial methanol cross-over still occurs. As a consequence, research is needed to discover membranes with lower methanol permeation, but due to the similar properties of methanol and water, methanol cross-over cannot be avoided completely. As an alternative way to solve the methanol cross-over problem methanol-tolerant catalysts can be used to avoid the formation of a mixed potential. Apart from that, alternative cathode catalysts with an improved oxygen reduction reaction compared to platinum would increase the efficiency of current generation. The investigation of new cathode catalysts has a high potential to improve DMFC, but a major problem of catalysts is their stability under fuel cell conditions.

The stability of the catalyst under these conditions is crucial for achieving operating times between several thousand and several ten thousand hours. To investigate the stability a combination of electrochemically in-situ

und physically ex-situ methods is necessary. During the lifetime of a fuel cell the electrochemical performance and the operation characteristics should not change significantly, therefore it is important that the hydrophobicity remains stable. Degradation of membrane electrode assemblies with platinum based catalysts has been investigated by many groups. Agglomeration of catalysts [1–4], mainly on the cathode side, is one main degradation process. A change of water balance and of transport processes in the electrode [5] caused by decreased hydrophobicity [6] were also identified as main degradation processes. This paper is focused on the physical characterization of different carbon-supported cathode catalysts based on platinum alloys and on noble-metal free catalysts like ruthenium-selenide and their stability during fuel cell operation.

2 Experimental

2.1 Sample preparation

2.1.1 Manufacture of electrodes and MEAs

Electrodes and membrane electrode assemblies (MEAs) were prepared with the DLR dry spraying technique [7–9]. The electrode powder is prepared by mixing the catalyst, PTFE or Nafion® powder (only for MEAs) for the reaction layer in a knife mill. In order to obtain homogeneous and thin reactive layers, the material is atomized and dry sprayed in a nitrogen stream through a slit nozzle directly onto the membrane. To improve electrical and ionic contact, the layer is fixed by hot rolling or pressing the membrane with gas diffusion layers (GDLs). By this production technique solvents are totally avoided and thin layers with thickness down to 5 µm can be prepared resulting in a low loading. For investigation of new catalysts the influence of the electrode structure should be minimized. Therefore, reaction layers have to be very thin. Although, thin layers with low catalyst loadings provide only a relatively low cell performance in DMFC, well-defined structures arise, which is an advantage for physical characterization. Besides this, an accelerated degradation of catalysts can be observed.

2.1.2 Catalysts for DMFC measurements

The following cathode catalysts were investigated in a DMFC single cell: Two different carbon-supported ruthenium-selenide catalysts supplied by project partners Hahn-Meitner-Institut (HMI) Berlin and Technische Universität München (TUM) and a carbon-supported platinum catalyst, which was defined as reference catalyst:

- 40 wt% RuSe/C with 26.0 wt% Ru, 13.4 wt% Se (supplied by TUM)
- 20 wt% RuSe/C with 18.7 wt% Ru, 0.9 wt% Se (supplied by HMI)
- 40 wt% Pt/C (reference catalyst).

Due to limitation in the amount of available experimental catalyst, the MEAs (Table 1) were prepared with low cathode loading, which is lower than the DLR standard loading for DMFCs (1.6 mg cm^{-2} for the anode (PtRu black) and for the cathode (Pt black)). Also, due to the material restriction, test electrodes could not be optimized with respect to electrochemical performance.

2.1.3 Catalysts for half-cell measurements

In order to test RuSe/C catalysts in a half-cell arrangement, gas diffusion electrodes (GDEs) were prepared with DLR dry spraying technique. Catalyst powder (without addition of electrolyte) was dry sprayed onto E-TEK carbon cloth. The catalyst with 20 wt% RuSe/C catalyst was used to prepare an electrode with a catalyst loading of 0.17 mg_{RuSe} cm^{-2}. As Pt reference catalyst an E-TEK single sided Elat electrode with 20 wt% Pt/Vulcan XC-72 with 0.4 mg cm^{-2} Pt loading and with 0.6–0.8 mg cm^{-2} Nafion® application was measured. For experiments a round piece with a diameter of 4 cm was cut from electrodes. Electrodes were cold-pressed with a Nafion® 117 membrane onto catalyst side of the electrode. GDEs were used as working electrode in half-cell arrangement with an apparent geometric surface area of 1 cm^2.

2.2 Physical characterization methods

Physical methods such as nitrogen adsorption (BET), porosimetry by mercury intrusion and temperature programmed reduction (TPR) were used to characterize the catalysts. To perform a complete surface science analysis

Table 1 Composition of MEAs for DMFC single cell measurements

Catalyst and metal content	Metal loading, content of electrolyte
Anode: PtRu black (JM)	1.00 mg_{PtRu} cm^{-2} + 30 wt% Nafion®
Cathode	
40 wt% Pt/C (Ref. catalyst)	0.10 mg_{Pt} cm^{-2} + 20 wt% PTFE
20 wt% RuSe/C (HMI)	0.14 mg_{RuSe} cm^{-2} + 20 wt% PTFE
40 wt% RuSe/C (TUM)	0.13 mg_{RuSe} cm^{-2} + 20 wt% PTFE
Membrane	Nafion® 117
GDL	E-TEK single sided ELAT V3
Active area; single meander flow field	23 cm^2

by X-ray photoelectron spectroscopy (XPS), the catalysts were studied before and after operation in fuel cells, respectively, after electrochemical treatment.

2.2.1 *Porosimetry measurements (N_2-adsorption, Hg-porosimetry)*

The pore systems, which are the crucial factors for transport mechanism and structure of electrodes, can be investigated by nitrogen adsorption (BET) [10] and mercury porosimetry [11, 12]. Nitrogen adsorption measurements were performed with a Sorptomatik 1990 device from Fision Instruments. These measurements yield information about micro- and meso-pore systems, which are mainly dominated by carbon supports. The specific surface area of complete samples—catalyst particles and carbon support—can be determined by nitrogen adsorption. For the investigation of meso- and macro-pores mercury penetration was used with PASCAL 140 and PASCAL 240 devices from Fision Instruments up to pressures of 2,000 bar. The macro-pore system is mainly determined by pores in the gas diffusion layer. Furthermore, with mercury penetration measurements the porosity can be directly determined. For investigation of catalysts, porosimetry measurements on catalyst powders were performed.

2.2.2 *Temperature programmed reduction (TPR)*

TPR experiments were performed in a TPDRO 1100 device from Thermoelectron [13]. In TPR measurements the consumption of hydrogen used for reducing the catalyst is measured during heating of the sample. From the consumed hydrogen the amount of oxide can be determined. The strength of oxide binding is calculated from the reduction temperature. Therefore, TPR provides information about stability of oxides. For avoiding influence of PTFE, only catalyst powders were investigated.

2.2.3 *X-ray photoelectron spectroscopy (XPS)*

The chemical composition of first atomic layers determines catalytic behavior. X-ray photoelectron spectroscopy yields information about element concentration and chemical binding state of the elements at sample surfaces (over a thickness of some atomic layers). For XPS, samples are irradiated by X-rays of characteristic photon energy in ultrahigh vacuum. The energy of photoelectrons, which are emitted from sample surface, is determined in an energy analyzer [14, 15]. XPS measurements were performed with an ESCALAB 250 from Thermoelectron equipped with a non-monochromatic dual anode X-ray gun and a hemispherical analyzer. Catalyst powders were analyzed by XPS before the electrochemical stressing, cathodes before and after the electrochemical stressing. Anodes were also examined for investigating whether components of the cathode catalyst have moved to the anode side during electrochemical stressing. Electrodes were obtained from MEAs after separation of electrodes from the membrane and were cut by a scalpel. Electrodes from half-cell experiments were cut by scissors. All electrodes were dried in the sample lock-in under vacuum conditions.

2.3 Electrochemical characterization methods

MEAs were electrochemically characterized by *V–i* characteristics and electrochemical impedance spectroscopy (EIS) [16] in a DMFC. Cathode catalysts were electrochemically investigated in half-cell experiments by steady state and cyclic voltammetric measurements.

2.3.1 *Direct methanol fuel cell (DMFC) measurements*

Electrochemical characterization of MEAs was performed in a single DMFC with a single meander flow field and an active area of 23 cm^2. The fuel cell test setup was automated and controlled by a computer and a PLC [17]. EIS measurements were carried out with a Zahner-elektrik IM6 (Kronach, Germany) impedance device and a potentiostat PP200 from Zahner-elektrik. All data were collected and analyzed with "Thales" software from Zahner-elektrik. Impedance spectra were obtained by varying the frequency of the voltage perturbation signal from 100 mHz to 100 kHz at 800 mA, the AC perturbation was a 10 mV amplitude. Each single cell was operated under standard operating conditions: Methanol (1.5 M, 10 ml min^{-1}, 2.5 bar) and oxygen (600 scc min^{-1}, 3.0 bar) were fed into anode and cathode electrodes, respectively. During the electrochemical characterization, optimized operation conditions of the RuSe/C catalysts were established for anode flow (5 ml min^{-1}) and cathode flow (60 scc min^{-1} under dry and 180 scc min^{-1} under humidified operating conditions). During fuel cell operation the CO_2 content in the cathode exhaust gas was determined.

2.3.2 *Half-cell measurements*

Experiments were carried out in a polymethylmethacrylate half-cell [18], in 0.5 M H_2SO_4 solution, at room temperature. The apparent geometric surface area of the working electrode was 1 cm^2. As reference electrode an $Hg/HgSO_4$ electrode in 0.5 M H_2SO_4 was used, as counter electrode a Pt plate. A potentiostat PP200 from Zahner-elektrik (Kronach, Germany) was used for the steady state and cyclic voltammetric measurements. All data were collected and analyzed with "Thales" software from Zahner-elektrik.

3 Results and discussion

3.1 Physical characterization of carbon-supported platinum alloy catalysts

Platinum alloy catalysts for fuel cells have been investigated since the 1960s. Initially, research activities were focused on anode catalysts for DMFCs [19–22]. In the last years platinum alloy catalysts were investigated as cathode catalysts in PEFCs in order to improve the oxygen reduction reaction (ORR). Due to the noble metal character of platinum the dissociation of oxygen molecules in acid media is a sluggish process, which is accelerated if the formation of oxides on the cathodic catalyst is improved. Therefore, platinum alloy catalysts with a reduced noble metal behavior are interesting, especially alloys with transition metals. Various alloys were tested by catalyst manufacturing companies like Johnson Matthey [23]. Not only wasan improved ORR reported but also an enhanced stability of some alloy catalysts compared with earlier use of pure platinum catalysts. The particle size of the alloy catalysts is higher compared to the particle size of pure platinum catalyst. It is a well-known effect that larger particles are more stable compared to small particles.

Tenside stabilized alloy catalysts represent an attractive alternative if they have a higher reactivity for oxygen reduction compared to platinum. For PtCo, PtCr and PtNi alloys a higher activity for ORR compared to pure platinum catalysts and a good stability was reported [24–28]. At DLR different carbon-supported Pt-alloy catalysts (PtMe/C; Me = Cr, Co, Ni), provided by Forschungszentrum Karlsruhe (FZK), were investigated physically by Hg-porosimetry, BET, TPR and XPS:

- 42.3 wt% Pt_3Ni/C
- 42.3 wt% Pt_3Co/C
- 30.0 wt% PtCr/C
- 40.0 wt% Pt/C (reference catalyst).

3.1.1 Hg-porosimetry and BET measurements of PtMe/C catalysts

Two different pore structures were found for the catalysts (Fig. 1a and b). A pore structure of 30–50 nm predominates in the catalyst with 30.0 wt% PtCr/C (by Hg-porosimetry), whilst the catalysts with 42.3 wt% Pt_3Ni/C, 42.3 wt% Pt_3Co/C and 40 wt% Pt/C show a pore size distribution at approximately 2 nm (by BET). The pore system of supported catalysts and their specific surface is mainly dominated by carbon support. The pore system at 30–50 nm is characteristic for Vulcan XC-72 carbon black. For the Pt_3Ni/C, the Pt_3Co/C and the Pt/C catalyst a carbon support with very small pore radius was used, which may affect the activity of the Pt-alloy catalyst in a negative way because of lack of accessibility of catalyst particles in very small pores.

By comparing the values for the specific surface area as well as the values for the porosity determined by mercury penetration, use of different carbon supports was confirmed. The carbon support of the PtCr catalyst has a lower specific surface as well as a significant lower porosity. All data obtained from Hg-porosimetry and N_2-adsorption are summarized in Table 2.

Porosity and pore size distribution can strongly influence the utilization of catalysts and the turn over frequencies, because in very small pores both are limited by transport processes. Therefore, the pore diameter has to be large enough for mass transfer. In addition, the catalyst should be deposited on the outer surface of the carbon support not in the pores. Hence, carbon supports with lower porosity and lower specific surface area are more suitable for catalyst preparation compared to supports with high porosity and very small pores. Decreasing catalyst utilization with increasing specific surface area is reported for DMFC anodes [29].

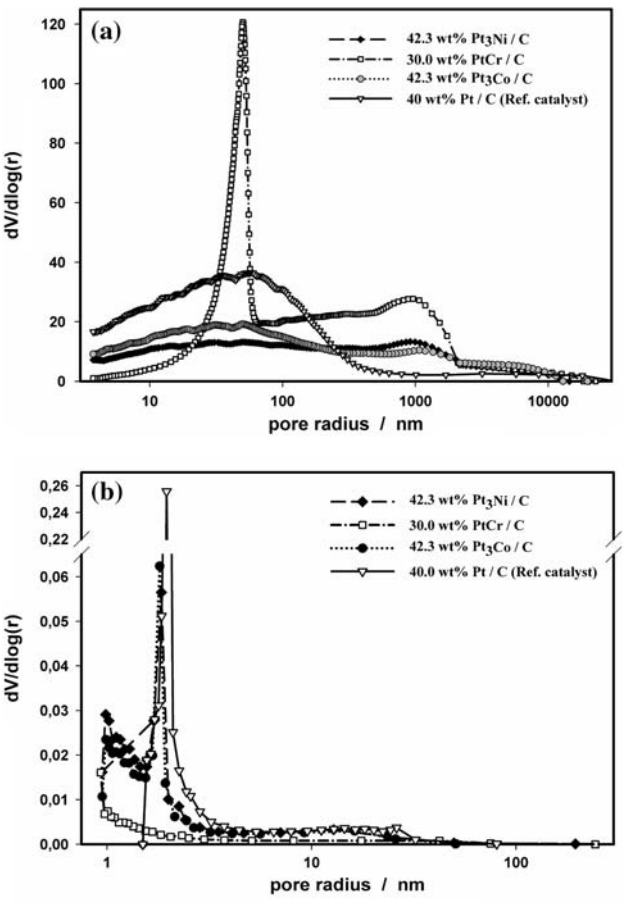

Fig. 1 (**a**) Hg-porosimetry and (**b**) BET spectra of PtMe/C and Pt/C catalysts

Table 2 TPR-, BET- and Hg-porosimetry data of PtMe/C and Pt/C catalysts

Catalyst	TPR-measurement		N_2-adsorption		Hg-porosimetry		
	Reduction temperature (1. Peak) (°C)	Reduction temperature (2. Peak) (°C)	Specific surface (m^2 g^{-1})	Pore radii (nm)	Specific surface (m^2 g^{-1})	Porosity (%)	Pore radii (nm)
30.0 wt% PtCr/C	380	480	123		58.9	29.9	53
42.3 wt% Pt_3Co/C	280	520	558	1.8	145	61	61
42.3 wt% Pt_3Ni/C	250	520	664	1.86	141	61	–
40.0 wt% Pt/C	480	–	762	2	150	76	71

3.1.2 Temperature programmed reduction (TPR) measurements of PtMe/C catalysts

In Fig. 2 TPR spectra of platinum alloy catalysts and the reference catalyst are displayed. Spectra were normalized with respect to the metallic content of the catalysts. Reduction temperatures are listed in Table 2. For each Pt-alloy catalyst two reduction peaks were recorded, for the Pt catalyst one reduction peak. It can be assumed that carbon-supported catalysts with a high Pt content have larger platinum particles sizes. Accordingly, it might be supposed that the peak at lower temperature in the TPR is related to surface oxides, whereas the high temperature peak to bulk oxides. But it may also be that the reduction temperatures reflect different oxides.

TPR spectra show that the catalysts with 42.3 wt% Pt_3Ni/C and 42.3 wt% Pt_3Co/C have similar reduction temperatures at the two maxima. The reduction temperature of the catalyst with 30.0 wt% PtCr/C is higher at the first peak but lower at the second. The reduction temperature reflects the strength of oxygen–metal binding of the alloy metal. The higher the reduction temperature the more stable are the oxides. Under same measurement conditions the reduction temperature for platinum black catalysts is significantly lower [30] compared to the reduction temperature for the alloy catalysts. Reduction of surface oxide or adsorbed oxygen on unsupported platinum takes place below room temperature.

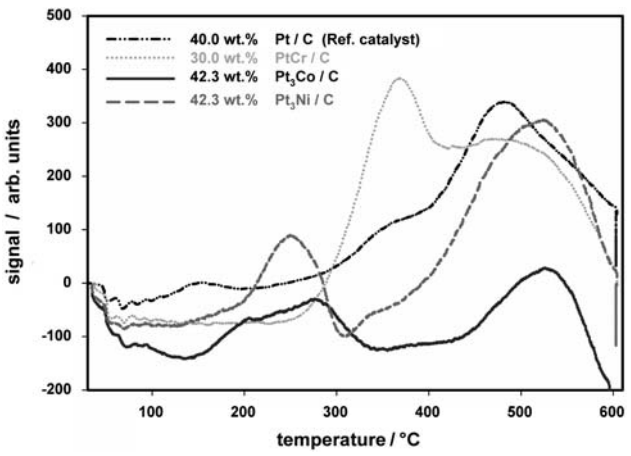

Fig. 2 TPR measurements of PtMe/C and Pt/C catalysts

3.1.3 X-ray photoelectron spectroscopy (XPS) investigations of PtMe/C catalysts

Figure 3a–d presents XP-spectra of the Pt-alloy catalysts. Signals were normalized to the same carbon signal intensity, because the atomic carbon concentration in the volume differs not significantly for the Pt-alloy catalysts; the volume atomic concentration of carbon is between 96 and 98% for the investigated catalysts. The most conspicuous result is that the surface concentration of the alloy catalysts does not correspond to the mixed ratio of the catalysts. A platinum-rich surface was found for the PtMe/C catalysts. The platinum concentration on surface of the 42.3 wt% Pt_3Ni/C and the 42.3 wt% Pt_3Co/C catalyst is in the same range, whereas the platinum concentration of the 30.0 wt% PtCr/C catalyst is considerable higher. Two different carbon supports were used (deduced by porosimetry measurements), which strongly effects the surface platinum concentration. The XPS result can be correlated to observations of porosimetry measurements that the use of nanoporous carbon support with micro-pore system at 2 nm leads to lower accessibility of platinum particles.

In addition to unexpected platinum concentration, the ratios of platinum concentration to alloy metal are also not consistent with the volume concentration, e.g. the ratio of platinum to cobalt in the Pt_3Co catalyst is different compared to the ratio of platinum to nickel in the Pt_3Ni catalyst, although for both catalysts the same ratio was expected. Additionally, the ratio of platinum to chromium is not 1:1. The alloy metals are in an oxidized state and not in metallic form. The analysis of the platinum alloy catalysts clearly shows that surface compositions of supported catalysts depend not only on the ratio of initial materials, but also on platinum support and the interaction of materials.

3.2 Physical characterization of RuSe/C catalysts

Over the past decade, different types of methanol-tolerant cathode catalysts have been developed to circumvent the

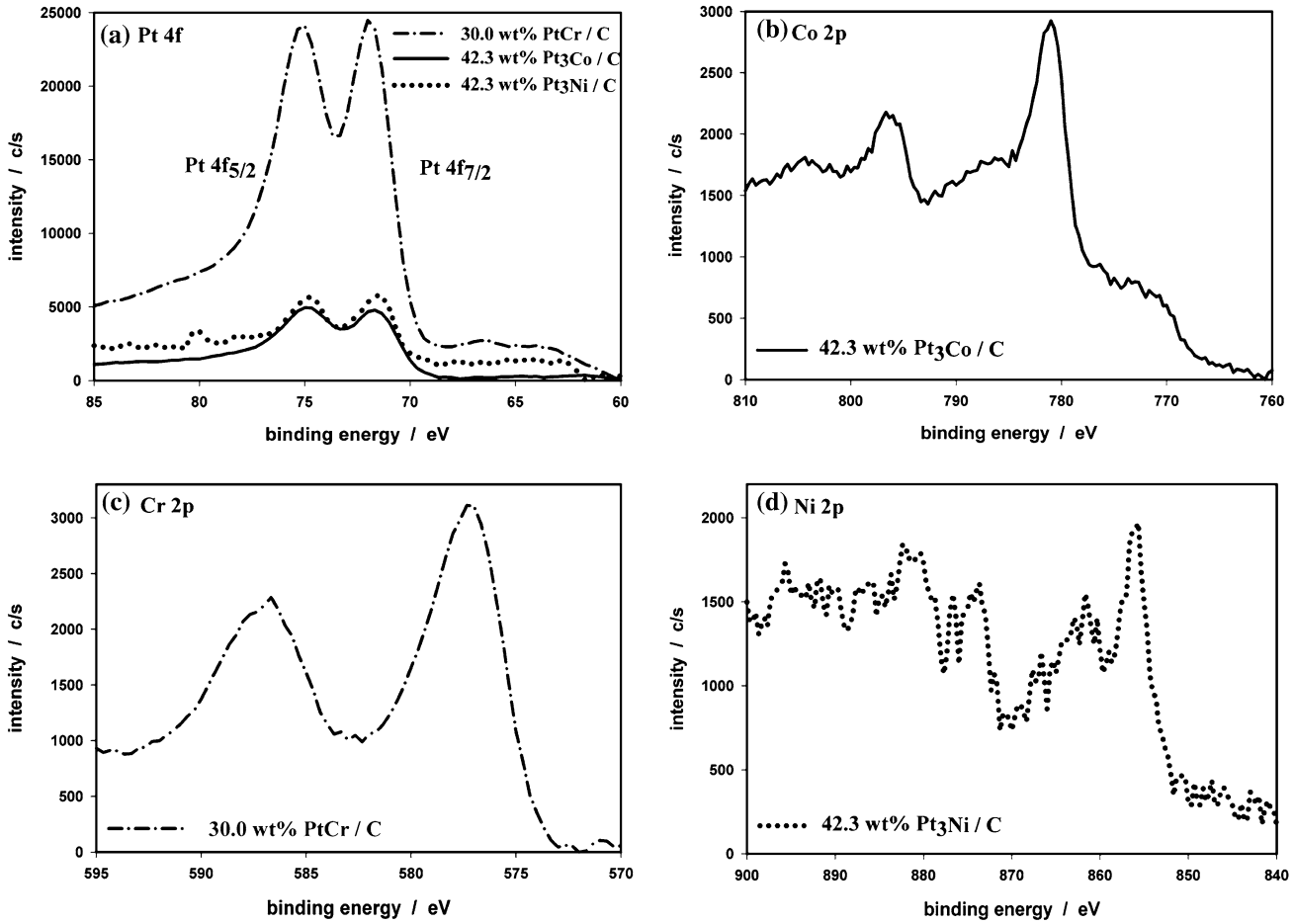

Fig. 3 XP-spectra of PtMe/C catalysts: (**a**) Pt 4f, (**b**) Co 2p, (**c**) Cr 2p, (**d**) Ni 2p

significant performance loss in DMFC caused by methanol oxidation. Platinum-free catalysts, such as ruthenium-selenide, have high reactivity with respect to the ORR and are insensitive to methanol oxidation [31, 32].

3.2.1 Hg-porosimetry and BET measurements of RuSe/C catalysts

Hg-porosimetry measurements of the carbon-supported RuSe-catalysts with 40 wt% RuSe and 20 wt% RuSe show a sharp peak in the pore size distribution at pore radii between 30 and 50 nm, which is typically for Vulcan XC-72 carbon. BET measurements confirm these results. All data are summarized in Table 3.

3.2.2 Temperature programmed reduction (TPR) measurements of RuSe/C catalysts

TPR spectra of the ruthenium-selenide catalysts are depicted in Fig. 4. The higher reduction temperature of the 40 wt% RuSe/C catalyst is attributable to the higher selenium to ruthenium ratio in the catalyst (26.0 wt% Ru, 13.4 wt% Se) compared to the ratio in the 20 wt% RuSe/C catalyst (18.7 wt% Ru, 0.9 wt% Se). The appearance of two reduction peaks for both ruthenium-selenide catalysts indicates the presence of two oxides. For the 40 wt% RuSe/C catalyst a peak is implied on the left shoulder at approximately 125 °C. The reduction temperatures are listed in Table 3.

3.3 Electrochemical characterization of RuSe/C catalysts

V–i characteristics of the MEAs with the 40 wt% and with 20 wt% RuSe/C cathode catalyst show a cell performance in the same range, which is significantly lower compared to cell performance of the MEA with the Pt/C reference catalyst. Low cell performance of MEAs with RuSe/C catalysts originates mainly from low catalyst loading, resulting in very thin electrodes, and partly from a lower activity of the RuSe/C catalysts compared to the platinum catalyst. Further reasons are: non-optimized operating conditions for RuSe/C and use of GDLs and cathode reaction layers, which are adapted for platinum catalysts. Hence, the non-optimized hydrophobic–hydrophilic properties of the

Table 3 TPR-, BET- and Hg-porosimetry data of RuSe/C and Pt/C catalysts

Catalyst	TPR-measurement		N_2-Adsorption		Hg-Porosimetry		
	Reduction temperature (1. Peak) (°C)	Reduction temperature (2. Peak) (°C)	Specific surface ($m^2\ g^{-1}$)	Pore radii (nm)	Specific surface ($m^2\ g^{-1}$)	Porosity (%)	Pore radii (nm)
20 wt% RuSe/C	80	120	135	58	74	56	42
40 wt% RuSe/C	–	154	104	41	55	66	39
40 wt% Pt/C	480	–	762	2	150	76	71

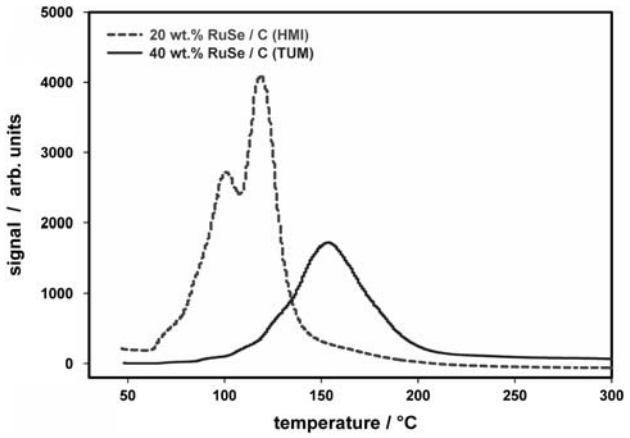

Fig. 4 TPR measurements of RuSe/C catalysts

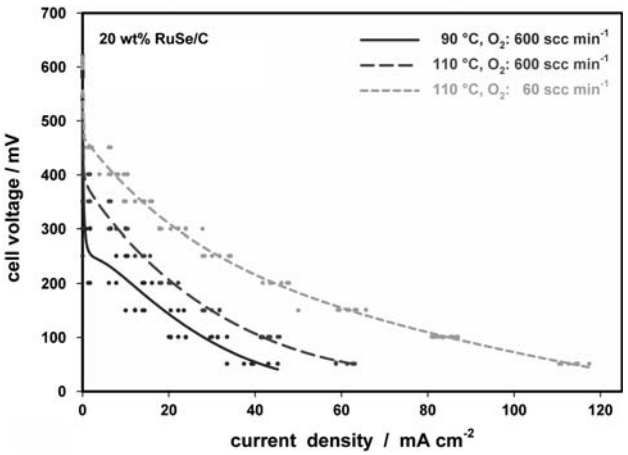

Fig. 5 *V–i* characteristics of 20 wt% RuSe/C catalyst under variation of cell temperature and cathode flow rate, 1st day

cathode reaction layer and related unfavorable water balance contribute to significantly lower cell performance for the RuSe/C catalysts. However, the aim of these investigations was to offer an insight into behavior and properties of ruthenium-selenide catalysts under DMFC conditions especially by varying operating conditions. Furthermore, we tried to ascertain if degradation effects occur.

In Fig. 5, *V–i* characteristics of the MEA with the 20 wt% RuSe/C catalyst at various oxygen flow rates and cell temperatures are depicted. Increase in cell temperature leads to a gain in cell performance caused by enhanced kinetics. Increase in cell performance by decreasing cathode flow rate indicates a different hydrophobic character of the RuSe catalyst compared to Pt or an improved water transport, resulting in more capable water removal from the cathode. The RuSe catalysts allow higher water content in the cathode. In the following experiments the cathode flow rate was set to 60 scc min^{-1}.

Previous measurements have shown a change in water balance from the 1st to the 2nd day (by shut-down over night) associated with an increased cell performance depending on the catalyst system. The same reaction can be seen in *V–i* characteristics of the RuSe/C catalysts, depicted for the 40 wt% RuSe/C catalyst in Fig. 6. An improved water balance is responsible for the general increase of cell performance for the RuSe/C catalyst. In contrast, the non-specific behavior of the Pt/C catalyst is attributed to non-optimized operating conditions for the platinum catalyst. At the second day a slight decrease for the RuSe/C catalyst by raising the cell temperature cannot be related to the cathode, because conditions for the cathode were optimized for the RuSe/C catalyst by reducing the cathode flow. Motivated by this effect, variation of anode flow rates was performed (Fig. 7). At a cell temperature of 110 °C the reduction of the methanol flow rate leads to an increase in cell performance, indicating an anodic effect on performance.

Investigating the influence of humidified cathode gas, the oxygen flow was humidified by passing the gas through a heated tank (bubbler) filled with water. Adjusting of humidity was done by controlling the water temperature in the humidifier (for a cell temperature of 90 °C at 70 °C, respectively for 110 °C at 90 °C). An increase in cell performance at 90 °C and at 110 °C by use of the humidified oxygen, associated with use of higher cathode flow without drying the cell, confirms the presumption of a different hydrophobic character of ruthenium-selenide compared to platinum.

By performing DMFC measurements it was obvious that the open circuit potential (OCP) of the MEA with the platinum cathode was higher than observed for MEAs with the RuSe/C catalyst. Additional half-cell experiments

Table 4 EIS data of the MEAs with RuSe/C and Pt/C catalysts

Operating conditions (at 800 mA)	20 wt% RuSe/C (HMI) (mV)	40 wt% RuSe/C (TUM) (mV)	40 wt% Pt/C (Ref. catalyst) (mV)
Comparison of cell voltage at different cell temperatures (90 °C, 110 °C)			
T-cell: 90 °C; cathode flow: 60 scc min^{-1}; anode flow: 10 ml min^{-1}, 1.5 M MeOH	200	150	490
T-cell: 110 °C, cathode flow: 60 scc min^{-1}; anode flow: 10 ml min^{-1}, 1.5 M MeOH	240	205	
Comparison of cell voltage at dry and humidified cathode flow			
T-cell: 90 °C, cathode flow: (dry) 60 scc min^{-1}; anode flow: 5 ml min^{-1}, 1.5 M MeOH		230	490
T-cell: 90 °C, cathode flow: (humid.) 180 scc min^{-1}; anode flow: 5 ml min^{-1}, 1.5 M MeOH		270	515
Comparison of cell voltage at different methanol concentrations			
T-cell: 90 °C, cathode flow: 60 scc min^{-1}; anode flow: 5 ml min^{-1}, 1.5 M MeOH		230	490
T-cell: 90 °C, cathode flow: 60 scc min^{-1}; anode flow: 5 ml min^{-1}, 4.5 M MeOH		220	450

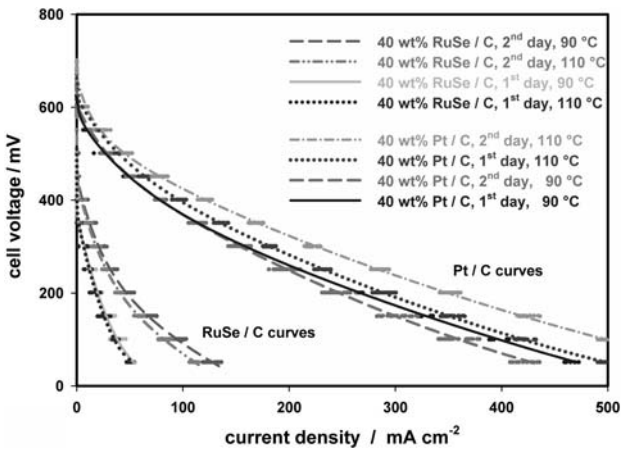

Fig. 6 Comparison of *V–i* characteristics of 40 wt% RuSe/C and 40 wt% Pt/C catalyst from 1st to 2nd day at 90 and 110 °C

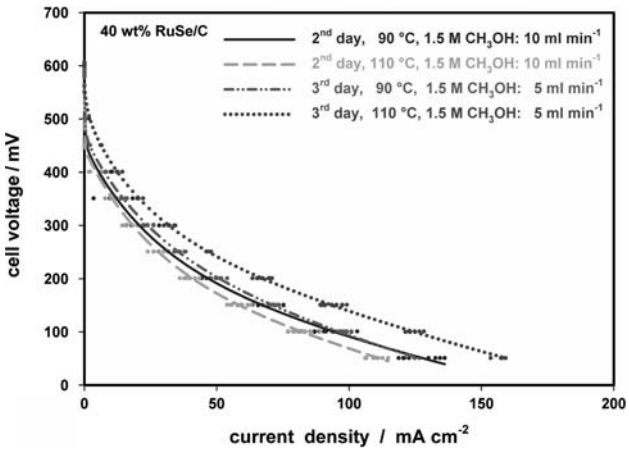

Fig. 7 *V–i* characteristics of 40 wt% RuSe/C catalyst under variation of anode flow rate, at 90 and 110 °C

confirmed this observation. Taking a closer look at changes in OCP (Fig. 8), a slight increase from the 1st to 2nd day for the MEA with the Pt/C catalyst in the DMFC and, in a more pronounced way in half-cell measurements, occurs. Whereas MEAs with the RuSe/C catalysts show a contradictory behavior, in the half-cell configuration a strong increase of OCP is observed. In DMFC the OCP increases at cell temperature of 90 °C, but decreases or remains unchanged at 110 °C. The strong increase in OCP for electrodes with the Pt/C and the RuSe/C catalyst in the half-cell configuration indicates the presence of a cleaning effect, taking place from the 1st to 2nd day. The raise of OCP for the MEA with the Pt/C catalyst during humidified operation and with use of higher cathode flow rate was caused by more favorably working conditions for the platinum catalyst. As expected, the OCP value for the electrode with platinum catalyst decreases significantly with addition of 1.5 M methanol in the half-cell experiment. The same behavior can be observed in DMFC by increasing the methanol concentration. In particular, the observed voltage drop of OCP for MEAs with RuSe/C catalysts, caused by the increase in methanol concentration, has to be emphasized. In conjunction with the unchanged behavior of the RuSe/C catalyst by addition of 1.5 M methanol in the half-cell experiment, it can be considered that an increase in methanol concentration influences the anode.

The contrasting results from half-cell experiments and from DMFC measurements cannot be explained only as an effect on the cathode side. The anode reaction has also been influenced by the different cathode catalysts. A possible reason is the formation of H_2O_2 on the cathode, which

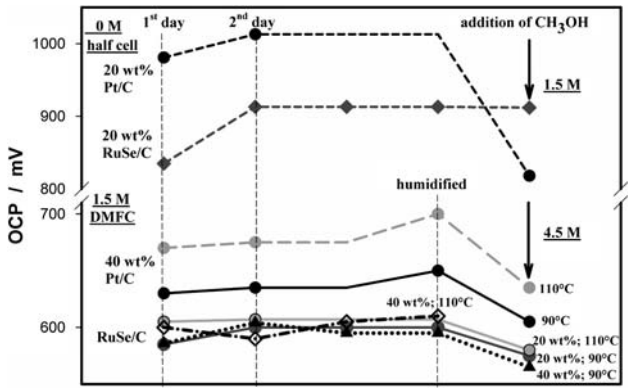

Fig. 8 OCP of RuSe/C and Pt/C catalysts, in half-cell experiments and DMFC

might pass through the membrane from cathode to anode side, resulting in a mixed anode potential and MEA degradation.

During DMFC measurements the CO_2 content at the cathode outlet was recorded and is displayed in Fig. 9. The CO_2 concentration at the cathode outlet was significantly higher at all operating conditions if platinum was used as cathode catalyst. For the MEA with the RuSe/C catalyst only a very low CO_2 concentration was observed. For the MEA with the platinum cathode the CO_2 concentration is approximately 2 vol% higher under DMFC operation compared to the value under OCP conditions, caused by methanol drag. Additionally, the CO_2 concentration increases with increasing methanol concentration and further with increasing cell temperature. In contrast, the CO_2 concentration for the RuSe/C catalyst was unaffected by operation conditions, as well as by methanol concentration. Under OCP conditions 0.0 vol% CO_2 was measured. Under load the CO_2 concentration increased to 0.1–0.2 vol% caused by CO_2 transport through membrane. The measurements confirm the methanol tolerance of RuSe/C catalysts. Methanol, which passes the membrane, was not oxidized on the RuSe/C catalyst. Recorded CO_2 concentrations for the RuSe/C cathodes originated from CO_2 cross-over from anode to cathode side.

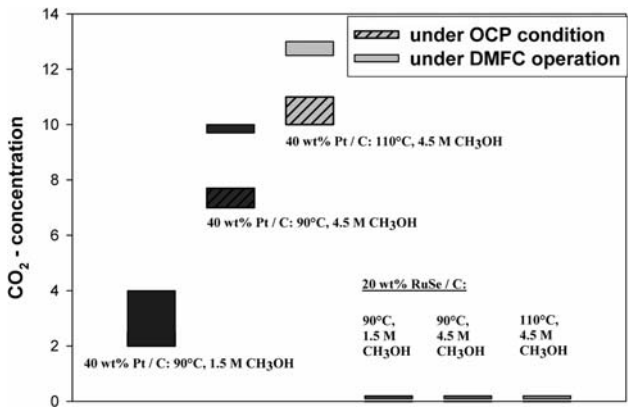

Fig. 9 CO_2 concentration of 20 wt% RuSe/C and 40 wt% Pt/C catalysts, under OCP conditions and under DMFC operation at various cell temperatures and methanol concentrations

Differences in EIS spectra are attributable to the cathode because the MEAs were prepared with the same membrane and anode composition. EIS spectra for MEAs with the RuSe/C catalyst show the same behavior (Fig. 10). From the low frequency region it can be concluded that the cell with the 40 wt% Pt/C cathode has the highest catalytic activity, and the lowest real value of impedance. The 20 wt% RuSe/C catalyst possesses a higher catalytic activity than the 40 wt% RuSe/C catalyst. Slight differences in the high-frequency region can only be explained by the different conductivity of the electrode material.

Nyquist plots (not shown here) show the typically behavior of DMFC cells. In the low frequency region the imaginary part of the resistance has positive values, which represents inductive behavior and can be described by relaxation impedance.

Impedance spectra of the 40 wt% RuSe/C catalyst, recorded under dry and humidified operating conditions, show a slight increase in cell performance caused by humidification of the cathode flow (Table 4). This corresponds to correlated *V–i* characteristics.

Triple-increase of methanol concentration has no notable influence on performance and impedance of the RuSe/C catalyst (Table 4).

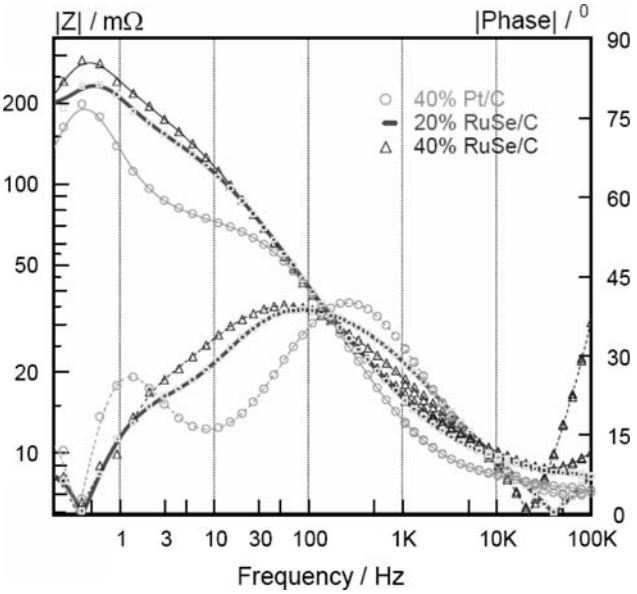

Fig. 10 EIS plots of RuSe/C and Pt/C catalysts, at 90 °C, 800 mA, 1.5 M MeOH

3.4 XPS postmortem investigations of RuSe/C catalysts

XPS investigations of cathodes before and after electrochemical stressing in DMFC were carried out. Spectra of Ru 3d and C 1s are depicted in Fig. 11. The Ru $3d_{5/2}$ peak (at a binding energy of 281 eV) indicates that ruthenium is present in both RuSe/C catalysts in an oxidized state, as RuO_2. After the electrochemical stressing a reduction of the ruthenium concentration in the 40 wt% RuSe/C catalyst can be observed. It can be assumed that a small contribution of ruthenium in the 40 wt% RuSe/C catalyst is present as ruthenium oxide without any quantities of Se and was removed from the surface during fuel cell operation.

Spectra of selenium of both RuSe/C catalysts differ (Fig. 12). No clear selenium peak was detected before the electrochemical stressing for the 20 wt% RuSe/C catalyst. The very low peak at 59 eV might be assigned to selenium oxide. In contrast, a definite Se 3d peak was measured in the sample after electrochemical stressing. This observation is attributed to a cleaning effect, which occurred during fuel cell operation. The low selenium oxide content

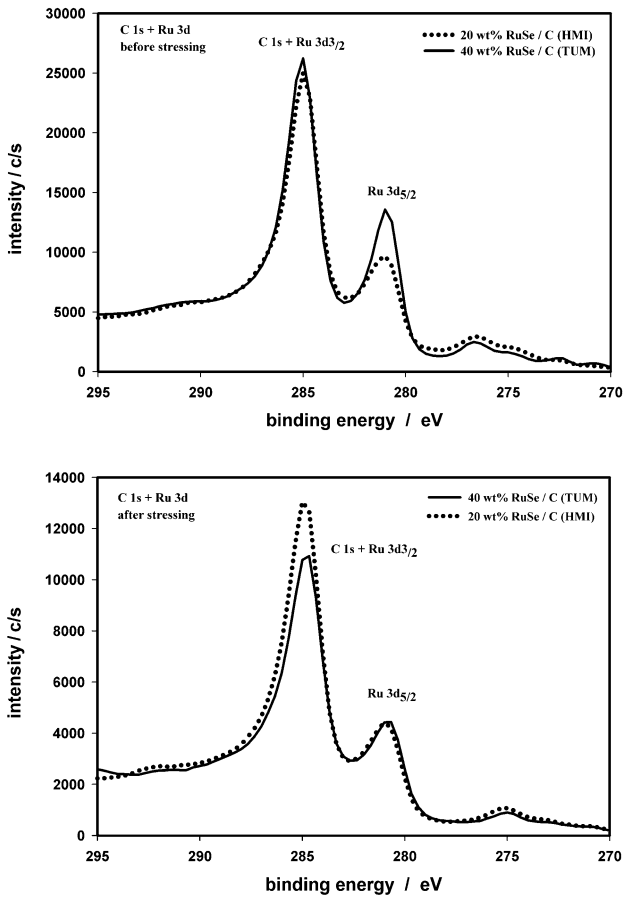

Fig. 11 XP-spectra of RuSe/C catalysts before and after electrochemical stressing: C 1s and Ru 3d peaks

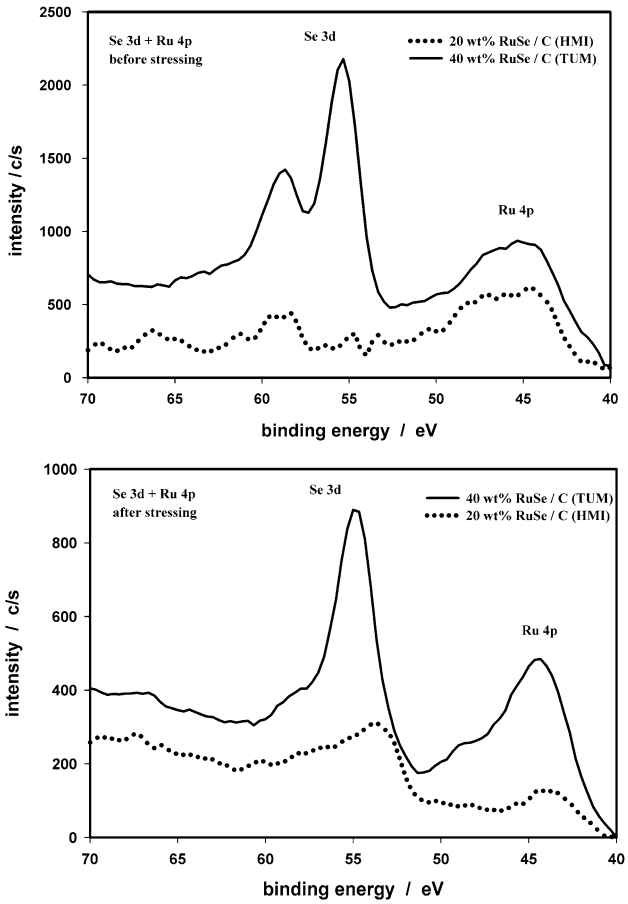

Fig. 12 XP-spectra of RuSe/C catalysts before and after electrochemical stressing: Se 3d and Ru 4p peaks

before electrochemical stressing is below the detection limit after operation.

In the 40 wt% RuSe/C catalyst, selenium can be observed in two different forms with binding energies at approximately 55 and 59 eV. The peak at higher binding energy can be assigned to selenium oxides, like SeO_2. The peak at lower binding energy can be assigned to metallic selenium and additionally to a selenide. The binding energies of elemental selenium and of the selenide are close to each other. For elemental selenium binding energies from 54.6 to 55.4 eV were recorded, for $RuSe_2$ a binding energy of 54.6 eV [33]. After DMFC operation a significant decrease of the selenium oxide peak is encountered. In conjunction with the decrease of the selenium oxide peak of the 20 wt% RuSe/C catalyst, it can be assumed that during fuel cell operation selenium oxide was removed from the catalyst surface to a large extent. The selenium oxide can be attributed to selenium, which is not bonded to ruthenium and is thus redundant. Selenium oxide is not electrochemically active as cathode catalyst. The ratio of the selenium/selenide to ruthenium increased during electrochemical stressing. Segregation of selenium in

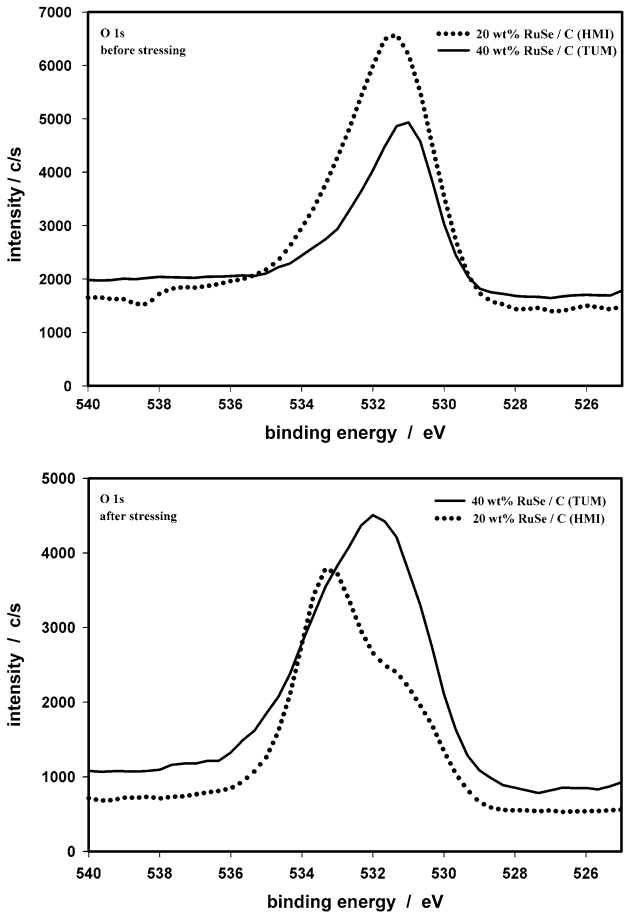

Fig. 13 XP-spectra of RuSe/C catalysts before and after electrochemical stressing: O 1s peak

ruthenium-selenide and its movement to the surface during fuel cell operation occurred.

Before electrochemical stressing, the asymmetrical peak of the O 1s spectra of the RuSe/C catalysts can be attributed to the convolution of two peaks. After electrochemical stressing the formation of a new feature in the O 1s spectrum of the 20 wt% RuSe/C catalyst was observed (Fig. 13) and can be explained by the presence of hydroxide groups. The peak at lower binding energy can be assigned to oxides.

4 Conclusions

The application of selected methods for physical and electrochemical characterization leads to useful results for further developments of new catalyst systems.

From XPS measurements, Hg-porosimetry and nitrogen-adsorption it could be concluded that surface composition of the investigated catalysts depends on support and preparation. Two different pore structures have been found for the Pt-alloy catalysts. In conjunction with XPS results it is proposed that the activity of the Pt-alloy catalysts, prepared with a carbon support with pore radii at 2 nm, might be affected in a negative way because of lack of accessibility of catalyst particles in the small pores.

TPR measurements yielded information on the stability of oxides. The higher reduction temperature of the 40 wt% RuSe/C catalyst can be attributed to the higher selenium to ruthenium ratio associated with higher oxide stability.

MEAs with the RuSe/C cathode catalysts were prepared and characterized in a DMFC single cell. By variation of cell temperature and of anode and cathode flow, optimized operating conditions of the RuSe/C catalysts were identified. The RuSe/C catalysts allow higher water content in the cell associated with an increase in cell performance. A change in the hydrophobic character of the RuSe/C catalysts occurred from the 1st to the 2nd day. In contrast to platinum, a significantly different hydrophobic behavior of the RuSe/C catalysts was found. Methanol tolerance of the RuSe/C catalysts was confirmed by variation of methanol concentration under simultaneous recording of CO_2 values in the cathode outlet. Low OCP values of RuSe/C could not be attributed solely to a cathode effect. It was presumed that the anode reaction was also influenced by the different cathode catalysts. The probable formation of H_2O_2 on the cathode, which passes through the membrane from cathode to anode side, resulted in a mixed anode potential. Decrease in OCP for MEAs with the RuSe/C cathode with increasing methanol concentration suggested that the Pt anode was affected. The unchanged OCP value for the RuSe/C catalyst, which was recorded with addition of methanol during half-cell measurements, confirmed this. Postmortem surface analysis by XPS showed that catalyst composition and MEA structure changed due to electrochemical stressing. The appearance of a cleaning effect during fuel cell operation was observed. Additionally, segregation of selenium in RuSe and its movement to the surface was measured. Furthermore, selenium oxide was removed from the surface of the catalysts to a large extent. For the 40 wt% RuSe/C catalyst a decrease in the ruthenium peak occurred.

Acknowledgements The authors address special thanks to colleagues for their supporting work. T. Kaz for preparation of the electrodes and MEAs, and I. Seybold for performing the half-cell experiments. The authors also wish to thank partners in the O_2RedNet-network for the supply of the catalysts: H. Bönnemann und K. Nagabhushana from the Forschungszentrum Karlsruhe (FZK). S. Fiechter, P. Bogdanoff, I. Hermann and I. Dorbandt from the Hahn-Meitner-Institut (HMI) Berlin. U. Stimming and A. Racz from the Technische Universität München (TUM). Funding by the network "Efficient Oxygen Reduction for the Electrochemical Energy Conversion—O_2RedNet", supported by the German Ministry of Education and Research is gratefully acknowledged.

References

1. Blurton KF, Kunz HR, Rutt DR (1978) Electrochim Acta 23:183
2. Staiti P, Arico AS, Antonucci V, Hocevar S (1998) J Power Sources 70:91
3. Schulze M, Schneider A, Gülzow E (2004) J Power Sources 127:213
4. Rice C, Tong Y, Oldfield E, Wieckowski A (1998) Electrochim Acta 43:2825
5. Schulze M, Wagner N, Kaz T, Friedrich KA (2007) Electrochim Acta 52(6):2328
6. Schulze M, Christenn C (2005) Appl Surf Sci 252:148
7. Gülzow E, Schulze M, Wagner N, Kaz T, Reissner R, Steinhilber G, Schneider A (2000) J Power Sources 86:352
8. Gülzow E et al (1999) Fuel Cells Bull 15:8
9. Bevers D, Gülzow E, Helmbold A, Müller B (1996) Innovative production technique for PEFC electrodes. In: Proceedings of the fuel cell seminar, Orlando, p 668
10. Gregg SJ, Sing KSW (1982) Adsorption, surface area and porosity. Academic Press, London
11. Carlo Erba Microstructure Line (1987) No. 5, p 1
12. Carlo Erba Microstructure Line (1987) No. 19, p 2
13. Webb PA, Orr C (1997) Analytical methods in fine particle technology. Micromeritics Instrument Corporation, ISBN 0-9656783-0-X
14. Henzler M, Göpel W (1991) Oberflächenphysik des Festkörpers. Teubner Studienbücher, Stuttgart
15. Ertl G, Küppers J (1985) Low energy electron and surface spectroscopy. VCH-Verlagsgesellschaft, Weinheim
16. Büchi FN, Gupta B, Haas O, Scherer GG (1995) Electrochim Acta 40:345
17. Gülzow E, Weißhaar S, Reissner R, Schröder W (2003) J Power Sources 118:405
18. Wagner N, Schulze M, Gülzow E (2004) J Power Sources 127:264
19. Vielstich W (1965) Brennstoffzellenelemente. Verlag Chemie GmbH, Weinheim
20. Binder H, Köhling A, Sandstede G (1972) In: Sandstede G (ed) From electrocatalysis to fuel cells. University of Washington Press, Seattle
21. Marković NM, Ross PN Jr (2002) Surf Sci Rep 45:117
22. Page T, Johnson R, Holmes J, Noding S, Rambabu B (2000) J Electroanal Chem 485:34
23. Ball SC, Hudson LS, Theobald BRC, Thompsett D (2006) Oxygen reduction catalysts for Automotive PEMFCs. 2. Workshop O_2RedNet, 06.–07. April, Ulm, Germany
24. Colón-Mercado HR, Popov BN (2006) J Power Sources 155:253
25. Travitsky N, Ripenbein T, Golodnitsky D, Rosenberg Y, Burshtein L, Peled E (2006) J Power Sources 161:782
26. Antolini E, Salgado JRC, Gonzalez ER (2006) J Power Sources 160:957
27. Yu P, Pemberton M, Plasse P (2005) J Power Sources 144:11
28. Colón-Mercado HR, Kim H, Popov BN (2004) Electrochem Commun 6:795
29. Rao V, Simonov PA, Savinova ER, Plaksin GV, Cherepanova SV, Kryukova GN, Stimming U (2005) J Power Sources 145:178
30. Schulze M, Gülzow E, Steinhilber G (2003) Characterization of catalysts for low temperature fuel cells with chemisorption, temperature programmed reduction and oxidation measurements. Fuel Cell Seminar, 03.–07. Nov 2003, Miami Beach, Ext. Abstract, p 307
31. Neergat M, Leveratto D, Stimming U (2002) Fuel Cells 2:25
32. Alonso-Vante N (2006) Fuel Cells 6:182
33. Schulenburg H, Hilgendorff M, Dorbandt I, Radnik J, Bogdanoff P, Fiechter S, Bron M, Tributsch H (2006) J Power Sources 155:47